REPORT SD-TR-81-62

LEVEL II

12

Voltage Losses and Reconditioning of NiCd Cells: Behavior During Cycling

A. H. ZIMMERMAN and M. C. JANECKI
Chemistry and Physics Laboratory
Laboratory Operations
The Aerospace Corporation
El Segundo, Calif. 90245

21 August 1981

Prepared for

SPACE DIVISION
AIR FORCE SYSTEMS COMMAND
Los Angeles Air Force Station
P.O. Box 92960, Worldway Postal Center
Los Angeles, Calif. 90009

This report was submitted by The Aerospace Corporation, El Segundo, CA 90245, under Contract No. F04701-80-C-0081 with the Space Division, Deputy for Technology, P.O. Box 92960, Worldway Postal Center, Los Angeles, CA 90009. It was reviewed and approved for The Aerospace Corporation by S. Feuerstein, Director, Chemistry and Physics Laboratory. Lt James C. Garcia, SD/YLVS, was the project officer for the Mission-Oriented Investigation and Experimentation (MOIE) Program.

This report has been reviewed by the Public Affairs Office (PAS) and is releasable to the National Technical Information Service (NTIS). At NTIS, it will be available to the general public, including foreign nations.

This technical report has been reviewed and is approved for publication. Publication of this report does not constitute Air Force approval of the report's findings or conclusions. It is published only for the exchange and stimulation of ideas.

James C. Garcia, 1st Lt, USAF
Project Officer

Florian P. Meinhardt, Lt Col, USAF
Director, Directorate of Advanced
Space Development

FOR THE COMMANDER

Norman W. Lee, Jr., Colonel, USAF
Deputy for Technology

UNCLASSIFIED

SECURITY CLASSIFICATION OF THIS PAGE (When Data Entered)

REPORT DOCUMENTATION PAGE	READ INSTRUCTIONS BEFORE COMPLETING FORM
1. REPORT NUMBER: SD-TR-81-62	2. GOVT ACCESSION NO.: AD-A105 418
	3. RECIPIENT'S CATALOG NUMBER
4. TITLE (and Subtitle): VOLTAGE LOSSES AND RECONDITIONING OF NiCd CELLS: BEHAVIOR DURING CYCLING	5. TYPE OF REPORT & PERIOD COVERED
	6. PERFORMING ORG. REPORT NUMBER: TR-0081(6970-01)-4
7. AUTHOR(s): Albert H. Zimmerman and Melanie C. Janecki	8. CONTRACT OR GRANT NUMBER(s): F04701-80-C-0081
9. PERFORMING ORGANIZATION NAME AND ADDRESS: The Aerospace Corporation, El Segundo, Calif. 90245	10. PROGRAM ELEMENT, PROJECT, TASK AREA & WORK UNIT NUMBERS
11. CONTROLLING OFFICE NAME AND ADDRESS: Space Division, Air Force Systems Command, Los Angeles, Calif. 90009	12. REPORT DATE: 21 August 1981
	13. NUMBER OF PAGES: 35
14. MONITORING AGENCY NAME & ADDRESS (if different from Controlling Office)	15. SECURITY CLASS. (of this report): Unclassified
	15a. DECLASSIFICATION/DOWNGRADING SCHEDULE

16. DISTRIBUTION STATEMENT (of this Report)

Approved for public release; distribution unlimited

17. DISTRIBUTION STATEMENT (of the abstract entered in Block 20, if different from Report)

18. SUPPLEMENTARY NOTES

19. KEY WORDS (Continue on reverse side if necessary and identify by block number)

Nickel-Cadmium Cell
Nickel Electrode
Phase Transformation
Reconditioning

20. ABSTRACT (Continue on reverse side if necessary and identify by block number)

The voltage losses that accompany the cycling of NiCd satellite cells are studied under a variety of operational conditions. The recovery of these losses through reconditioning procedures involving complete cell discharge is also examined. The results indicate that the voltage losses arise from a combination of thermodynamic and kinetic changes in the Ni electrode and that these changes result from a solid-state phase transformation in the Ni electrode active material.

DD FORM 1473 (FACSIMILE)

UNCLASSIFIED

SECURITY CLASSIFICATION OF THIS PAGE (When Data Entered)

CONTENTS

I. INTRODUCTION..... 5

II. EXPERIMENTAL METHODS..... 9

III. RESULTS..... 11

IV. DISCUSSION OF RESULTS..... 27

V. CONCLUSIONS..... 33

REFERENCES..... 25

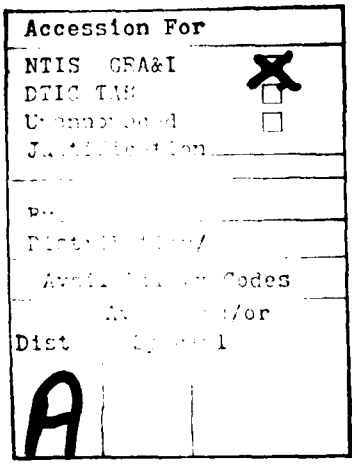

FIGURES

1. Discharge characteristics of NiCd cell after reconditioning and after 37 cycles; 4-A discharge (1 h), 2.5-A charge (1.28 h), 1-A charge (1.6 h) for each cycle..... 12

2. NiCd voltage loss during cycling..... 14

3. Voltage loss as a function of depth-of-discharge for discharge at 4 A and 0.5 A after 37 cycles as indicated in Fig. 1..... 15

4. Dependence of voltage loss on discharge current after 22 cycles employing 4-Ah discharge, followed by 1 A charge for 5 h..... 16

5. Development of voltage loss with cycling for a NiCd cell at several discharge currents..... 18

6. Development of voltage loss with cycling for a NiCd cell at several charge currents..... 20

7. Dependence of voltage loss on the charge current used during cycling; after 12 cycles and after 29 cycles..... 21

8. Dependence of voltage loss on overcharge..... 22

9. Development of voltage loss for cycling to various depths-of-discharge..... 23

10. Development of voltage loss with cycling in a 1 Ah NiCd cell at the Ni electrode and Cd electrode..... 25

11. Pictorial representation of how a phase separation may occur in the Ni electrode upon cycling..... 28

I. INTRODUCTION

Nickel cadmium battery cells are widely used in applications that require a large number of charge-discharge cycles. In satellite power systems NiCd batteries may experience thousands of charge-discharge cycles during the lifetime of the satellite. Any significant changes that occur in battery voltage or capacity characteristics over this lifetime must be compatible with the satellite power requirements and the battery power control unit capabilities. The most immediate change that often occurs in the NiCd cell as it is cycled is a steady decline in the voltage that the cell maintains during discharge. Such a loss of voltage puts an additional load on the batteries, and may in some cases cause a substantial loss in usable capacity. It has been empirically found for NiCd cells that a reconditioning procedure is effective in restoring the performance that is lost as a result of this short-term voltage degradation.[1] Reconditioning typically involves a deep discharge of the cell capacity at a very low rate followed by a full recharge.

The mechanisms that contribute to degradation of the voltage characteristics of NiCd cells and the recovery of the voltage on reconditioning are not well established. Mechanisms that tend to involve either physical or chemical changes at the cell electrodes have been discussed in the literature as contributing to voltage losses. Significant changes in the sizes and distribution of crystals of Cd and $Cd(OH)_2$ in the Cd electrode have been observed[2-4] as the electrode is cycled or aged. In these situations voltage losses could result from additional overpotentials due to decreased active Cd surface area (higher current densities). For positive limited cells, however, the preponderance of experimental data available indicates the positive electrode as most likely to undergo voltage degradation with cycling. Besides a very gradual swelling with age, there is little physical evidence for major structural changes in the Ni electrode. However, Jasinski[5] has proposed that Ni electrode voltage degradation on cycling results from slow annealing of the defect structure in the uncycled positive active material (NiOOH). The defect structure of the NiOOH is expected to be significant because the charge trans-

fer reaction rate is thought to be controlled by proton transport through the NiOOH lattice.[6,7]

The work of Bode and Dehmelt[8] gave the first characterization of the reactions taking place in the Ni electrode. They found charge transfer reactions occurring between several different phases of NiOOH and $Ni(OH)_2$:

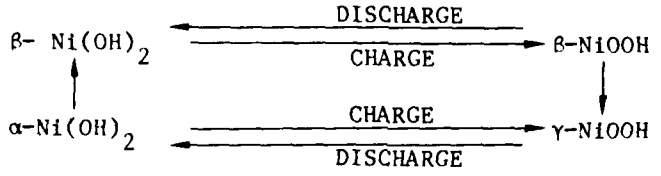

(1)

Since this work, a number of workers have studied the electrochemical and physical properties of the various Ni hydroxide-oxyhydroxide phases and the transitions that may take place between them. Milner and Thomas[9] and more recently Barnard et al.[10] have discussed the electrochemical behavior of these phases by treating them as solid solutions of Ni species in differing oxidation states. Both Harivel et al.[11] and Tuomi[12] have claimed that the discharge efficiency of γ-NiOOH is poor, and therefore that it only undergoes substantial discharge at low rates. However, in the recent work of Barnard et al.[13] the γ-NiOOH phase was found to undergo efficient high-rate discharge, albeit at potentials slightly lower than for the β-NiOOH. In addition, they attribute a second Ni electrode discharge plateau that is often seen about 300 mV below the primary discharge plateau to the removal of Ni^{+3} or Ni^{+4} defects from the $Ni(OH)_2$ as this material is discharged toward the divalent state.[10,13] The practical impact of these processes on the operation of the sealed aerospace NiCd cell has yet to be determined.

The changes in voltage characteristics that occur in aerospace NiCd cells during cycling and as a result of reconditioning must be considered both in the design of the battery power and charge control units, and in battery sizing and qualification. The magnitude of the voltage degradation may in some cases be obtained from life test data, if such test results are available for the operating conditions of the system in question. With such data the

conditions of battery charge, discharge, storage, and reconditioning may be optimized to some extent to minimize battery voltage degradation. Here we report measurements of voltage losses for NiCd cell operation in a variety of cycling modes for typical ranges of currents and temperatures. These data should provide inputs of use in designing the battery charge control unit and more importantly should serve as inputs in designing battery tests. In addition, the results should help settle some of the questions that remain concerning the major mechanisms for short-term voltage degradation and reconditioning in aerospace NiCd cells of the design studied here.

II. EXPERIMENTAL METHODS

The NiCd cells used in these experiments were 10 Ah nameplate, 12.6 Ah actual (at C/2 rate) capacity sealed cells of prismatic design, and manufactured by G.E. Three cells were used, all of which had Cd added to the Ni electrodes as an antipolar mass. The cells were about 8 years old and had experienced fewer than 1000 deep discharge cycles. Approximately 500 to 1000 cycles were added during the experiments reported here. No changes in either performance or discharge voltage characteristics could be attributed to aging of the cells during these experiments. The voltage changes observed during cycling were reproducible among the three cells used.

The cells were restrained from expanding by 0.25-in. aluminum plates bolted to the sides. Two connectors were soldered to each of the cell electrode posts, allowing the voltage monitoring leads to be separated from the current-carrying leads. The cells were charged and discharged at constant current. The cycling was accomplished by a battery cycler, constructed in our laboratory, which controlled the conditions of charge, discharge, and open-circuit stand. The open-circuit stand during cycling was kept to 1 sec except in situations where the effects of longer open-circuit periods were being investigated. The cell voltages were monitored at all times on a strip chart recorder that could be read with an uncertainty of about ± 2 mV. Some of the later data were taken with a data logger that had an uncertainty of ± 0.2 mV. The power supply used to charge and discharge the cells was a Kepco 36-15M. The amount of charge or discharge was determined either by the product of time and current, or in some cases by direct coulometric integration, and was accurate to ± 0.001 Ah. All experiments were at ambient temperatures (23 ± 2°C).

The conditions employed as a standard procedure for reconditioning the cells consisted of discharging the cell through a 1Ω resistor (10Ω for the 1-Ah laboratory constructed cell) after discharging to 1.0 V at the C/4 rate. The resistor was left on the cell for at least 16 h, after which the cell voltage was less than 10 mV. The cell was then recharged at the C/10 rate for 16 h, after which cycling was begun.

For experiments employing a reference electrode, a NiCd cell was constructed from 1-Ni and 2-Cd plates that were removed from a 10-Ah cell. The plates were separated by a layer of nylon separator (Pellon 2505). The current collector tabs of the plates were spot welded to Ni foil, to which lengths of Ni wire were spot welded. The Ni wires passed out of the cell housing for connection to the power supply. The electrode assembly was housed in a Plexiglas container that was flooded with CdO-saturated 31% KOH electrolyte. The container was closed but not sealed, and was continuously purged with N. The capacity of the laboratory cell was about 1.25 Ah, or about 10% of the capacity of the 10 Ah aerospace cells. A 1-A/25-V operational amplifier galvanostat was used in charging and discharging this cell.

The reference electrode consisted of a Ag wire sealed into a polyethylene tube that passed through the top of the cell housing and was positioned to be adjacent to one of the Cd plates. The Ag wire was briefly oxidized by anodizing it with respect to the Cd electrode at a current density of about 1 mA/cm^2. It is likely that the Ag_2O formed on the silver wire slowly dissolved in the electrolyte, resulting in instabilities after several days. It was found that long-term stability could be maintained by supplying an anodic current of about 40 nA to the Ag electrode to compensate for the effective dissolution current. This procedure gave excellent long-term stability for the Ag/Ag_2O reference electrode with only a slight loss in accuracy. It was determined that the reference polarization gave overpotentials of only 2 to 3 mV, which were essentially constant for the duration of the experiments. Since the experimental measurements involved voltage differences, the overpotential from the reference had less than a $\pm$ 0.2 mV effect on the data, which is insignificant compared to the resolution used in recording the voltages.

III. RESULTS

Voltage loss (ΔV) is defined here as the difference between the cell discharge voltage immediately after the standard reconditioning procedure and the cell discharge voltage after cycling. The value of ΔV is a function of the cell state of charge and the number of postreconditioning cycles on the cell for any given set of cell operating conditions. In addition, for any specific state of charge and cycle number, ΔV may depend on the charge and discharge currents, temperature, depth of discharge (DOD) for previous cycles, and the extent of overcharge.

To adequately characterize the voltage losses that do take place, two general kinds of measurements have been made. First, the cycling parameters of charge current, discharge current, trickle charge rate, recharge ratio, and DOD were varied in systematic ways and the voltage loss was monitored as a function of number of cycles from 20 up to 200 cycles. Presumably each of these variables may in general affect the final state into which the cell is placed as a result of cycling. The second kind of measurements that we have made involve characterization of that state that is obtained as a result of cycling. Some of these measurements are reported here, in particular those characterizing the steady-state current dependence of the voltage loss and how this current dependence changes with DOD. Cell kinetics have also been measured as a function of DOD, and will be reported separately. In addition, some data were obtained for the voltage losses encountered in cycling Ni and Cd cell plates in a laboratory cell in which an Ag/Ag_2O reference electrode was used. These measurements allow the voltage losses to be separated into the contributions from the Ni and Cd electrodes.

Typical data indicating the voltage depression that is observed after 37 cycles (to 40% of nameplate DOD) are shown in Fig. 1. The cycling consisted of discharge at 4 A for 1 h, followed by charge at 2.5 A for 1.28 h, then charge at 1 A for 1.6 h. The final discharge after cycling in Fig. 1 was at 4 A, with the arrow indicating the DOD to which the cell was cycled. Upon reconditioning, the cell delivered about 1 Ah more capacity above 1.1 V;

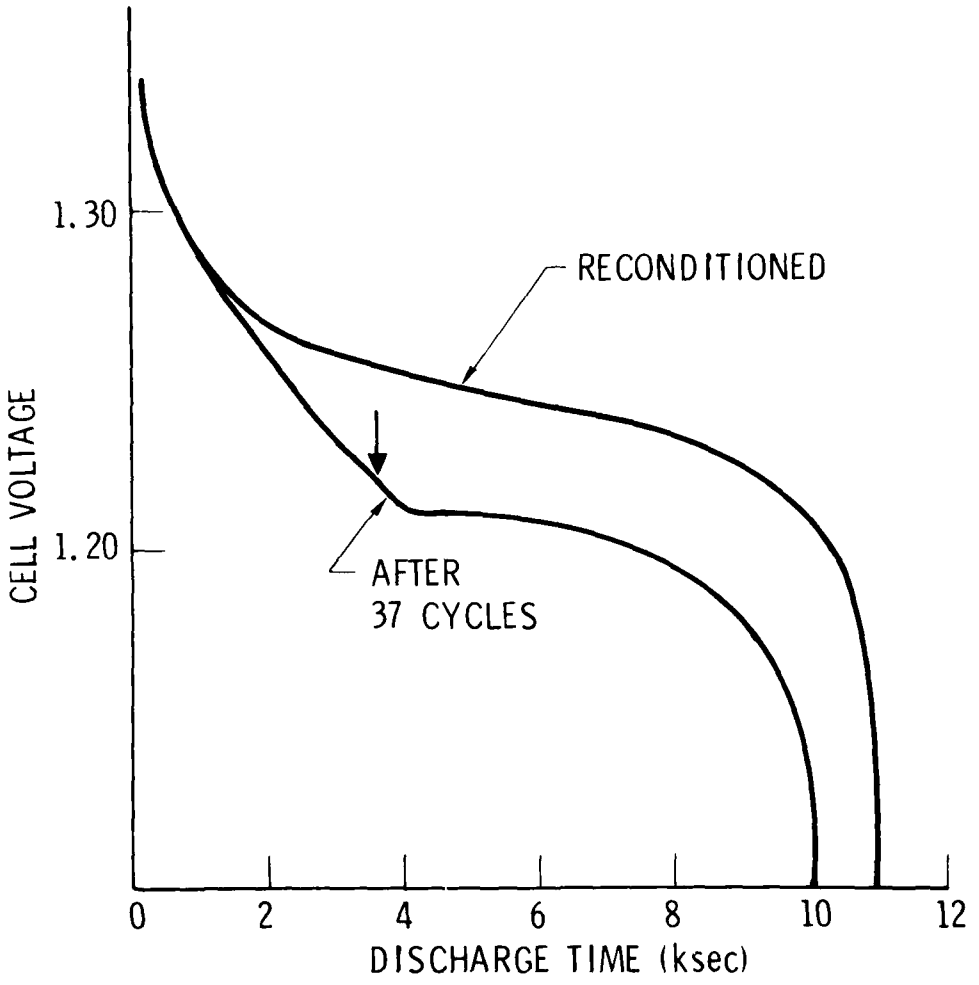

Figure 1. Discharge characteristics of NiCd cell after reconditioning and after 37 cycles; 4-A discharge (1 h), 2.5-A charge (1.28 h), 1-A charge (1.6 h) for each cycle. The arrow indicates the depth-of-discharge to which the cell was cycled.

however, when the residual capacity was discharged at 0.1 A to 0 V, the total available capacity was essentially the same for the cycled cell as it was for the reconditioned cell. Therefore, the differences between the discharge profiles in Fig. 1 are due to loss of cell voltage under load, rather than to any decrease in state of charge.

Figure 2 indicates how the loss of cell voltage in Fig. 1 develops during cycling at four DOD. Note that after about 10 to 15 cycles, no further voltage loss was observed during approximately the first half of each discharge cycle. As the DOD approached 40%, which was the capacity discharged during each cycle, a voltage loss component associated with long-term as well as short-term cycling was observed.

Figure 3 indicates the voltage loss as a function of DOD for the final discharge following 37 charge-discharge cycles. The cycling conditions are the same as described for the experiment in Fig. 1, except that curve A employed a 4-A final discharge current and curve B employed a 0.5-A final discharge current.

The data in Fig. 3 indicate substantial voltage losses even during discharge at a current as low as 0.5 A. This suggests that some of the voltage loss arises from thermodynamic changes (changes in open-circuit potential) in addition to the voltage losses from kinetic changes (overpotential, or rate-dependent voltage losses). The voltage losses from these two contributions may be described by

$$\Delta V = I_d \Delta R_{eff} + \Delta V_o \qquad (2)$$

where I_d is the discharge current, ΔV_o is the voltage loss at zero current, and ΔR_{eff} is the change in the steady-state cell polarization resistance at the discharge rate I_d. The value of ΔR_{eff} depends in general on I_d, as well as the conditions under which the cell was cycled prior to the final discharge. The two terms in Eq. (2) may be separated since ΔV_o is independent of current. This separation is indicated by curve C of Fig. 4, where ΔV is plotted as a function of I_d. The measurements indicated in curve C were made

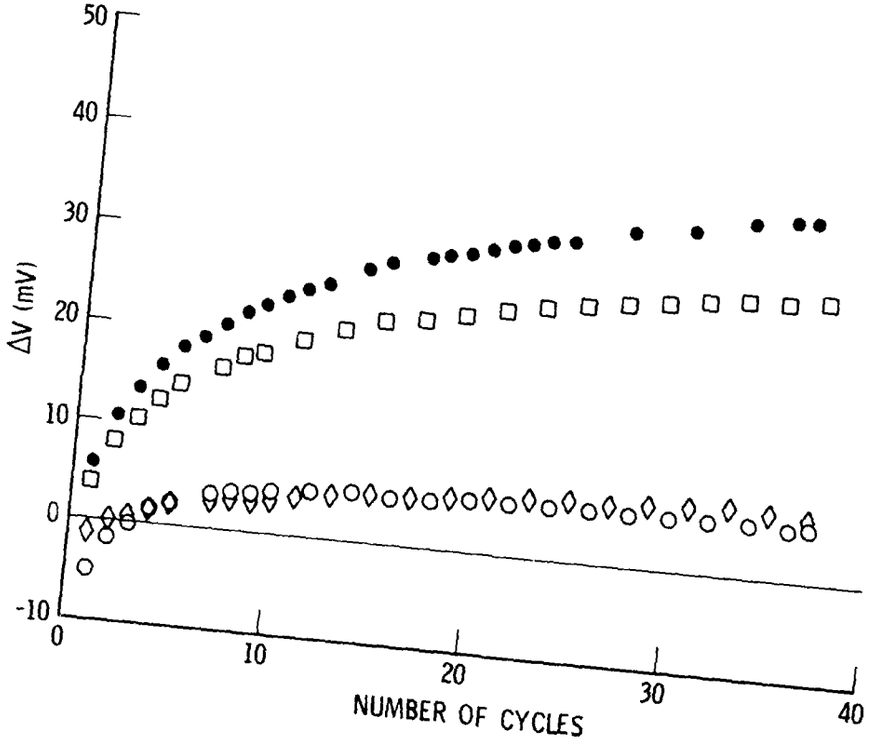

Figure 2. NiCd voltage loss during cycling. The data indicate how the difference between the two curves in Fig. 1 develops with cycling at 1 Ks (circles), 2 Ks (diamonds), 3 Ks (squares), and 3.6 Ks (points).

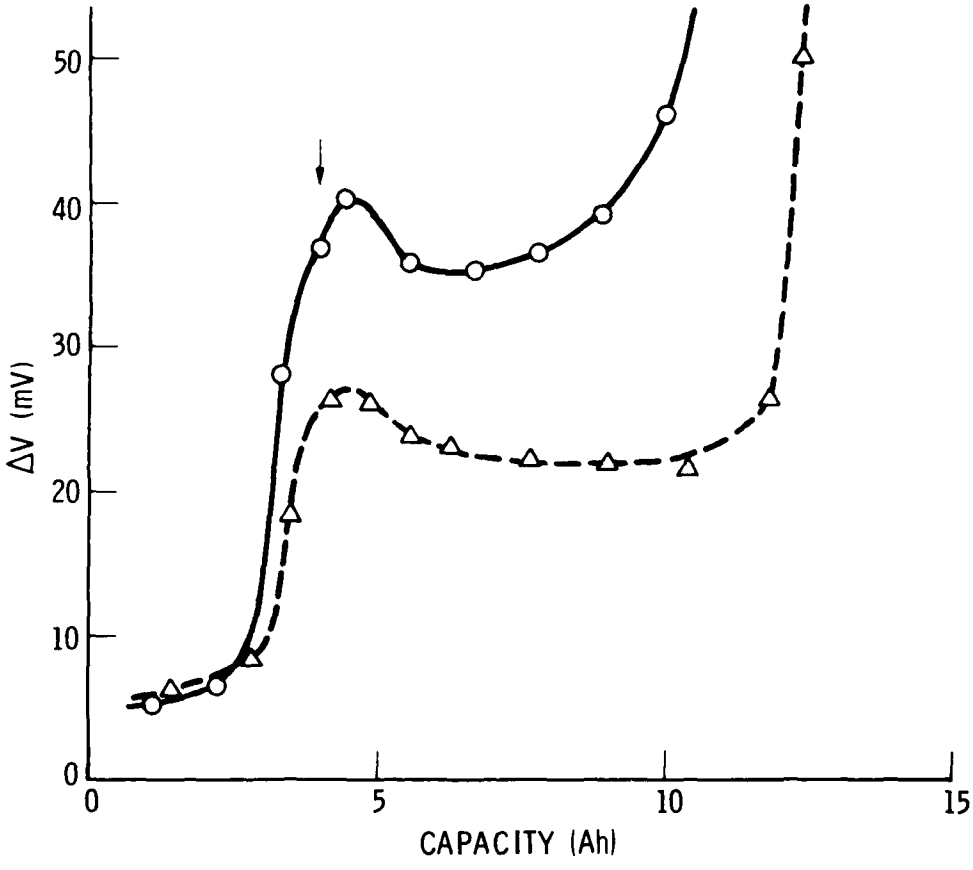

Figure 3. Voltage loss as a function of depth-of-discharge for discharge at 4 A (circles) and 0.5 A (triangles) after 37 cycles as indicated in Fig. 1.

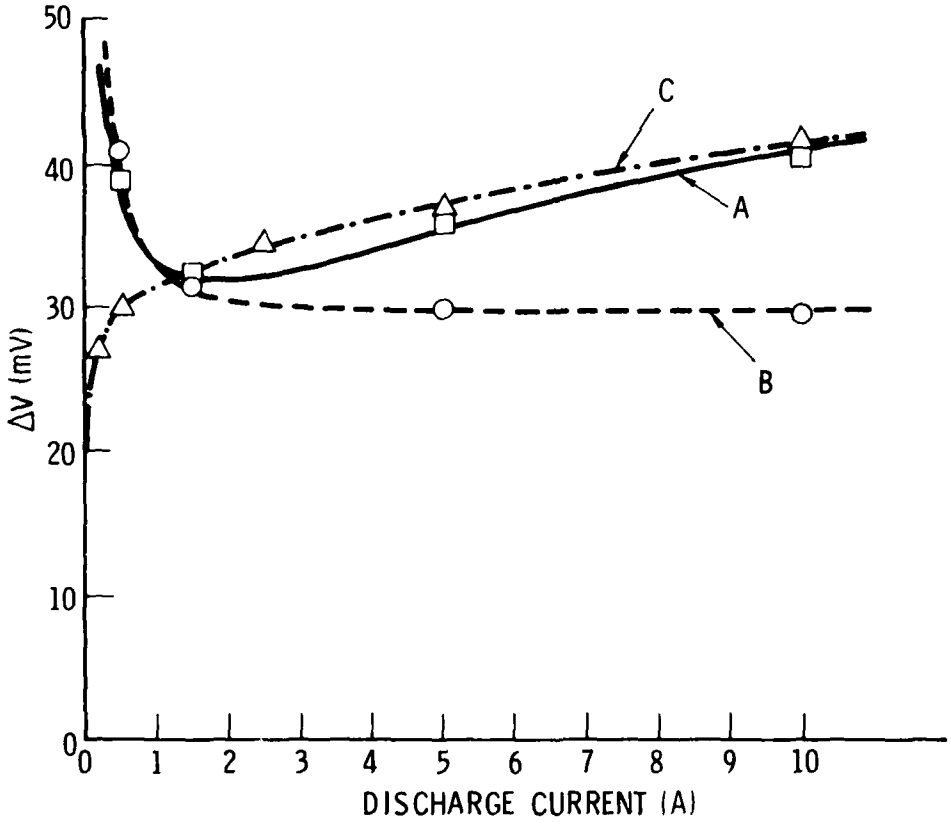

Figure 4. Dependence of voltage loss on discharge current after 22 cycles employing 4-Ah discharge, followed by 1-A charge for 5 h. For curve A the discharge current during cycling and during the final discharge was that indicated on the abscissa. Curve B involved cycling at the current on the abscissa followed by a 1-A final discharge. Curve C involves 22 cycles employing a 2.5-A discharge current, with the final discharge being at the current indicated on the abscissa.

by measuring ΔV at the peak indicated in Fig. 3, which was typically after 4.5 Ah of capacity had been discharged at the indicated rate, I_d. Before each ΔV measurement, the reconditioned cell was subjected to 22 cycles, each consisting of a 1-A charge for 5 h, followed by a 2.5-A discharge for 1.6 h. The point at zero current in curve C of Fig. 4 was obtained by discharging 4 Ah of capacity at 1.5 A after cycling, then allowing 20 h of open-circuit stand before measuring ΔV. Curve C of Fig. 4 is not linear, indicating that ΔR_{eff}, which is the slope of this curve, is itself current or rate dependent. Another significant result from this curve is that ΔV_o is about 20 mV, indicating a thermodynamic shift in the potential of the NiCd cell.

Repetitive cycling typically will change the chemical state of the NiCd cell as reflected by the changes in potential observed. The chemical state that is reached will in general depend on the discharge current used during the repetitive cycling. The experimental results indicated in curve B of Fig. 4 show ΔV as a function of the discharge current employed during the cycling. The cycling in these experiments involved 22 cycles, each consisting of charge at 1 A for 5 h, followed by discharge at the indicated current. In each experiment the value of ΔV was measured during the final discharge at the peak in ΔV (about 4.5 Ah discharged) during discharge at the 1-A rate.

The results indicated in curve A of Fig. 4 show the combined effects of the variables in curves B and C. For curve A the discharge current during cycling and the final discharge current were varied together, using the same cycling regime employed for the experiments indicated in curves B and C of Fig. 4. The result is a combination of the contributions to ΔV in curves B and C, causing curve A to have a minimum at an operating current of about 2 A.

The data presented in Fig. 5 indicate how ΔV develops during cycling at the different discharge currents employed. The cycling sequence was the same as described above for curve A of Fig. 4. The error bars on the points of Fig. 5 indicate the range of scatter in the data points. For Fig. 5 ΔV was measured after discharge of 4-Ah capacity at the indicated current, rather than at the peak of ΔV as in Fig. 4. For this reason the ΔV in Fig. 5 are smaller, particularly at a 10-A discharge current. This result suggests that

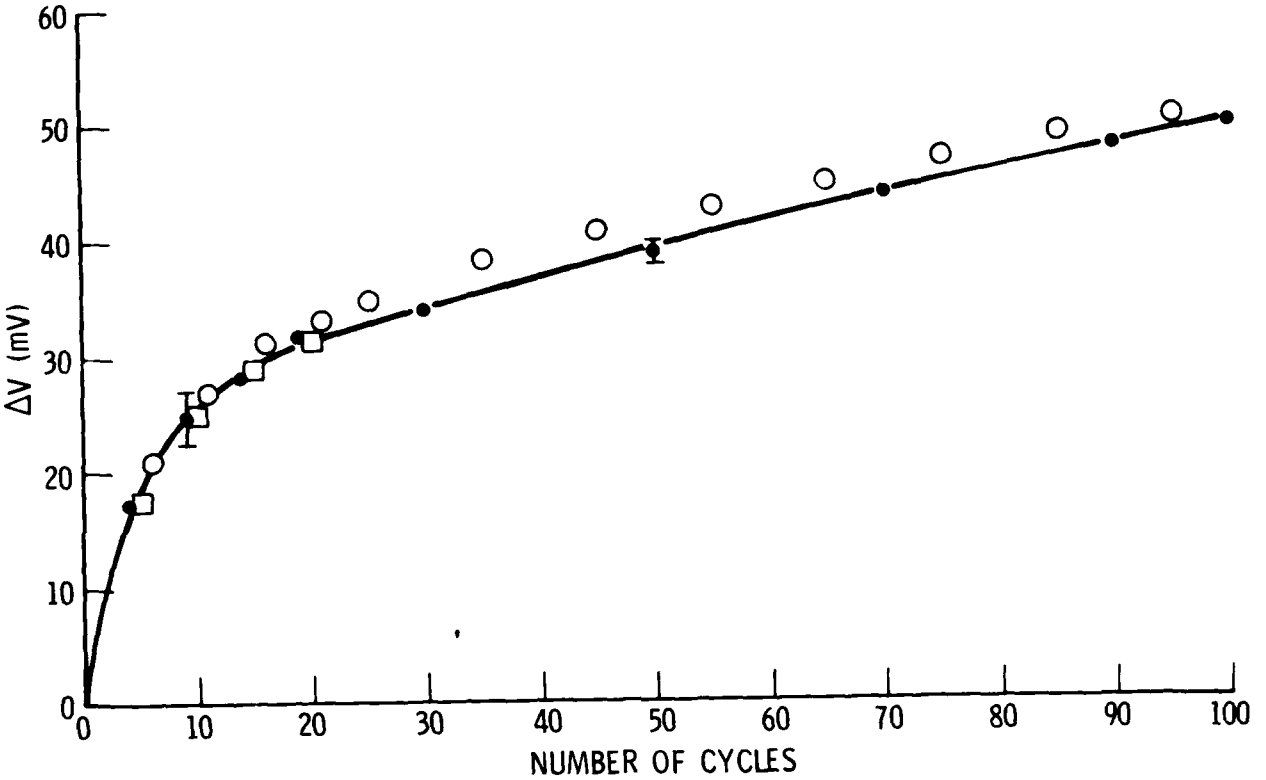

Figure 5. Development of voltage loss with cycling for a NiCd cell at several discharge currents. Each cycle employed 4 Ah of discharge, followed by 1-A charge for 5 h. The discharge currents are 1.5 A (circles), 5 A (points), and 10 A (squares).

in the region of 4 to 4.5 Ah DOD the value of R_{eff} in Eq. (2) is quite sensitive to the amount of capacity discharged, and that R_{eff} is substantially greater during discharge beyond the 4-Ah capacity.

The dependence of voltage losses on the charge rate during cycling is indicated in Fig. 6 for up to 30 cycles. The cycling sequence in these experiments consisted of discharging at 5 A until 4 Ah of capacity are discharged, charging at the specified rate until 80% of the charge is returned, then charging at 1 A until 125% of the charge is returned. In this way the overcharge duration and rate are essentially the same for all the experimental data shown in Fig. 6. The charge rates varied from 0.5 A to 5 A. The voltage losses on cycling show a quite pronounced dependence on the charge rate. This dependence is indicated in Fig. 7. At charge rates above 2.5 A the voltage loss is minimized and does not greatly depend on charge current; however, for charge rates below 2.5 A the voltage losses increase rapidly with decreasing current. From Fig. 6 the additional voltage loss that results from using a low charging current appears to become greater as the number of cycles increases, since the slopes of the ΔV plots become greater at the lower charging currents

The dependence of voltage losses on the extent of overcharge was also examined and is indicated in Fig. 8. For these experiments the cycle mode consisted of discharging at 5 A until 4 Ah of capacity were removed, recharge at 2.5 A to 80% charge return, followed by charging at 1 A until the indicated percentage charge return was obtained. Figure 8 indicates that for low percentages of charge return an increased loss of cell voltage is found after more than about 20 cycles. This may be caused by a somewhat lower average state of charge when only 105% charge return is used, since a slight decrease in capacity was noted when a low charge return was employed.

In Fig. 9 experimental results are presented that show how the voltage losses depend on the depth of discharge to which the cell is cycled. The cycling mode for these experiments consisted of discharging at 5 A to the indicated DOD based on nameplate capacity, recharging at 2.5 A until 80% of the charge was returned, then recharging at 1 A until 125% was returned. The

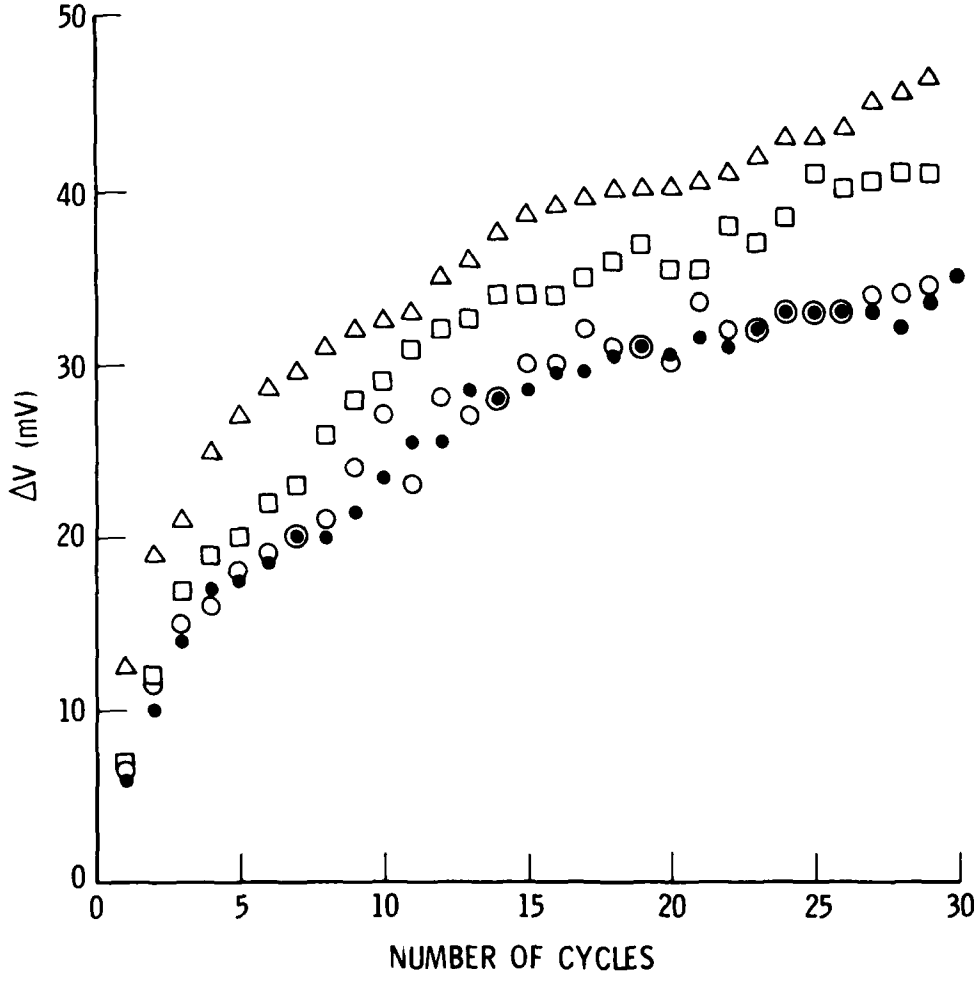

Figure 6. Development of voltage loss with cycling for a NiCd cell at several charge currents. Each cycle consisted of discharge at 5 A for 4 Ah, charge at the indicated current for 3.2 Ah, and charge at 1 A for 1.8 Ah. The charge currents are 0.5 A (triangles), 1.0 A (squares), 2.5 A (circles), and 5 A (points).

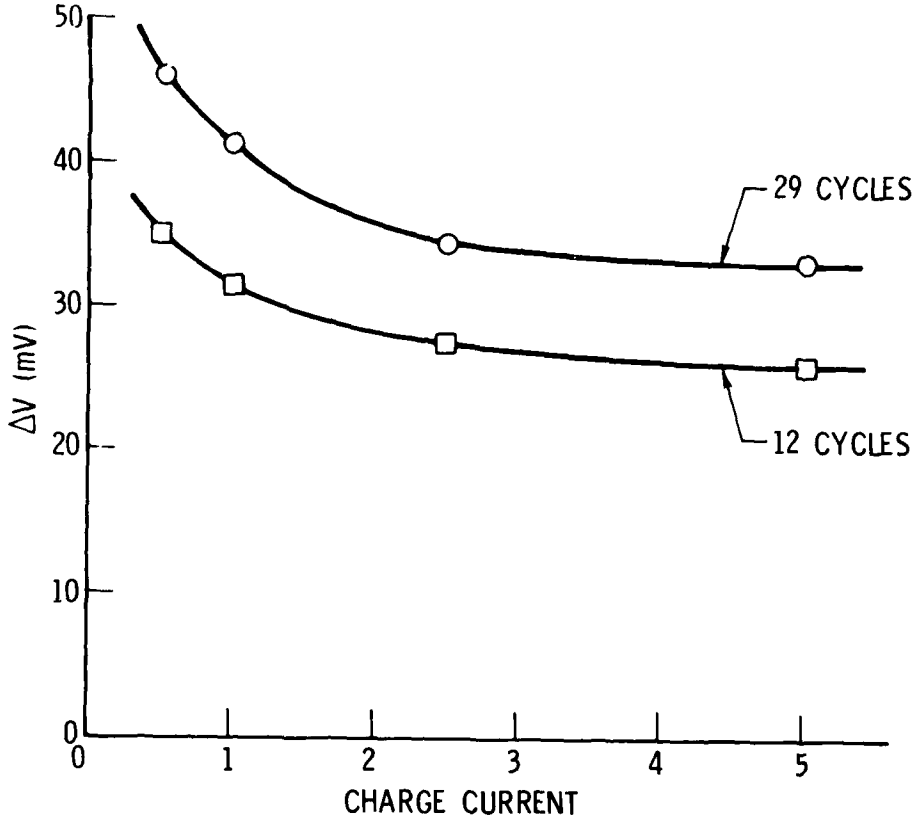

Figure 7. Dependence of voltage loss on the charge current used during cycling; after 12 cycles (squares) and after 29 cycles (circles). Each cycle involved a 5-A discharge for 4 Ah, followed by recharge at the current indicated on the abscissa for 3.2 Ah and then at 1 A for 1.8 Ah.

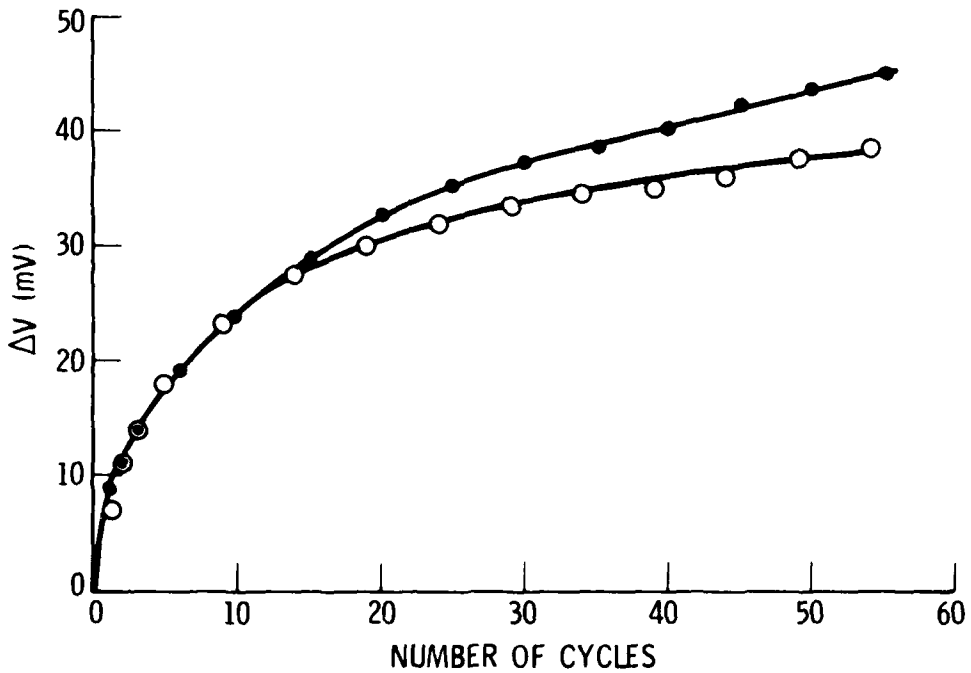

Figure 8. Dependence of voltage loss on overcharge. Each cycle involved a 5-A discharge for 4 Ah, followed by recharge at 2.5 A for 3.2 Ah and then at 1 A for 1 h (points, recharge ratio = 1.05) and at 1 A for 1.8 h (circles, recharge ratio = 1.25).

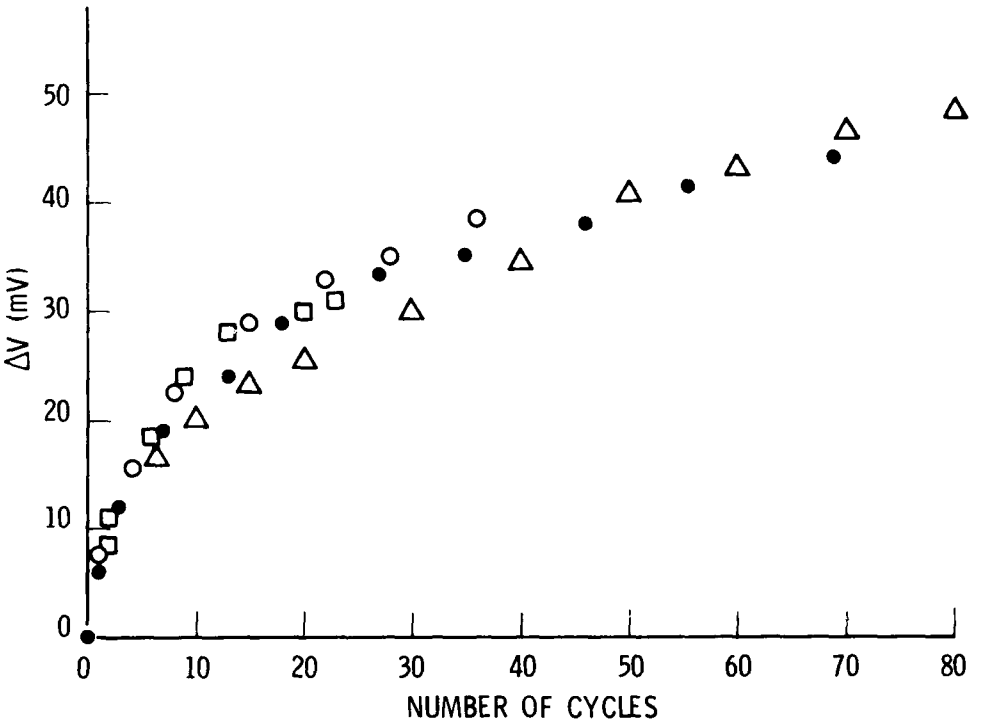

Figure 9. Development of voltage loss for cycling to various depths of dis charge. Each cycle involved discharge at 5 A for 1 Ah (triangles), 2.5 Ah (points), 5 Ah (circles), and 8 Ah (squares), followed by recharge at 2.5 A until 80% of the capacity discharged was returned, then recharge at 1 A until 125% of the capacity discharge was returned.

depths of discharge examined ranged from 10% to 80% of the 10-Ah nameplate value. The data in Fig. 9 indicate that there was very little dependence on DOD, but rather that the dominant factor in controlling voltage depression was the number of cycles on the cell.

Plates from a 10-Ah NiCd cell were cycled in an electrolyte-flooded laboratory cell that was equipped with an Ag/Ag_2O reference electrode that allowed the voltage losses from the individual Ni and Cd electrodes to be examined during cycling. This cell had approximately one-tenth the capacity of a 10-Ah cell. In this experiment the cycling mode consisted of discharge at 0.15 A until 0.4 Ah of capacity was discharged, followed by charge at 0.10 A until 115% charge was returned. The results are indicated in Fig. 10 for 22 cycles. The total loss in end-of-discharge voltage in Fig. 10 is very similar to the losses in sealed NiCd cells in Figs. 1-9. Essentially all of the voltage depression results from changes in the Ni electrode potential with cycling. The Cd electrode gave only a very slight voltage loss that was within the scatter of the data points in Fig. 10. These data suggest that the voltage losses indicated in Figs. 1 through 9 represent changes in the Ni electrode potential.

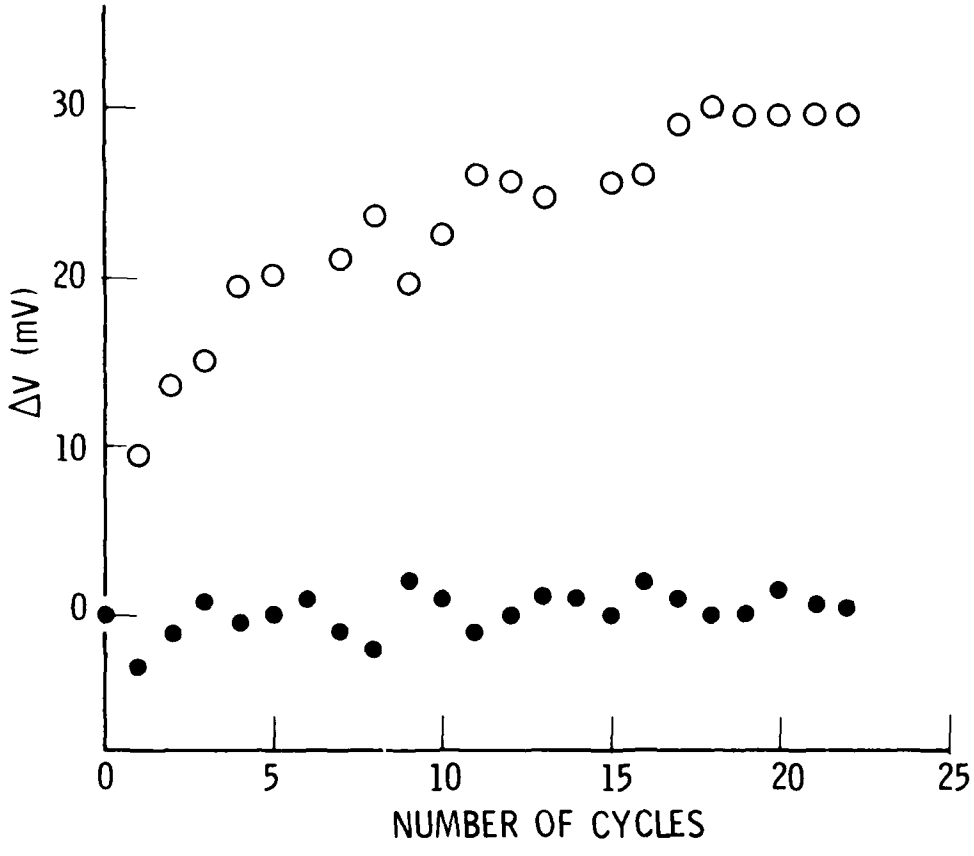

Figure 10. Development of voltage loss with cycling in a 1-Ah NiCd cell at the Ni electrode (circles) and Cd electrode (points). The reference electrode was Ag/Ag_2O. Each cycle involved discharge at 0.15 A for 0.4 Ah followed by recharge at 0.10 A for 0.46 Ah.

IV. DISCUSSION OF RESULTS

The results that have been obtained in this work may be most easily discussed in the framework of a reaction sequence such as that described in Eq. 1. Evidence for a reaction sequence of this general type for the Ni electrode has been previously given by other workers.[8,10,14,15] The most detailed scheme is that of Barnard et al.,[10,14] who found evidence for the charged β and γ phases of nickel oxyhydroxide, which may discharge to activated or deactivated β and activated or deactivated α phases, respectively. In addition, conversion of the charged β phase to the charged γ phase is possible during charge, and conversion of the discharged α phase to the discharged β phase is possible during discharge or open circuit. A reconditioning discharge in this scheme may be regarded as conversio. of active material to a deactivated β phase that is then recharged to the active β-NiOOH.

A model of how the phase composition of the Ni electrode might change during the course of cycling is represented pictorially in Fig. 11. From the reconditioned or completely discharged state the cell is initially recharged predominantly to β-NiOOH. Discharge of this material forms β- $Ni(OH)_2$* that is then recharged during cycle 2 to form some γ-NiOOH as well as β-NiOOH. On each subsequent cycle the β-NiOOH is discharged preferentially over the γ-NiOOH, while more γ-NiOOH is formed during each recharge. Eventually a steady state is reached when the amount of γ-NiOOH generated during recharge balances that which is reduced during discharge. The two-phase system leads to a discharge voltage for the cycled cell, such as that in Fig. 1, which consists of two regions. The higher potential region occurs during preferential discharge

*The discharged material is referred to as $Ni(OH)_2$ in this report for convenience. The work of Barnard et al.[10,11] suggests that the active material actually discharges initially to a phase having an oxidation state on the order of 2.25. Subsequent low-rate discharge may further discharge this phase towards the divalent state at potentials 300 to 400 mV lower than the normal Ni electrode potential during discharge.

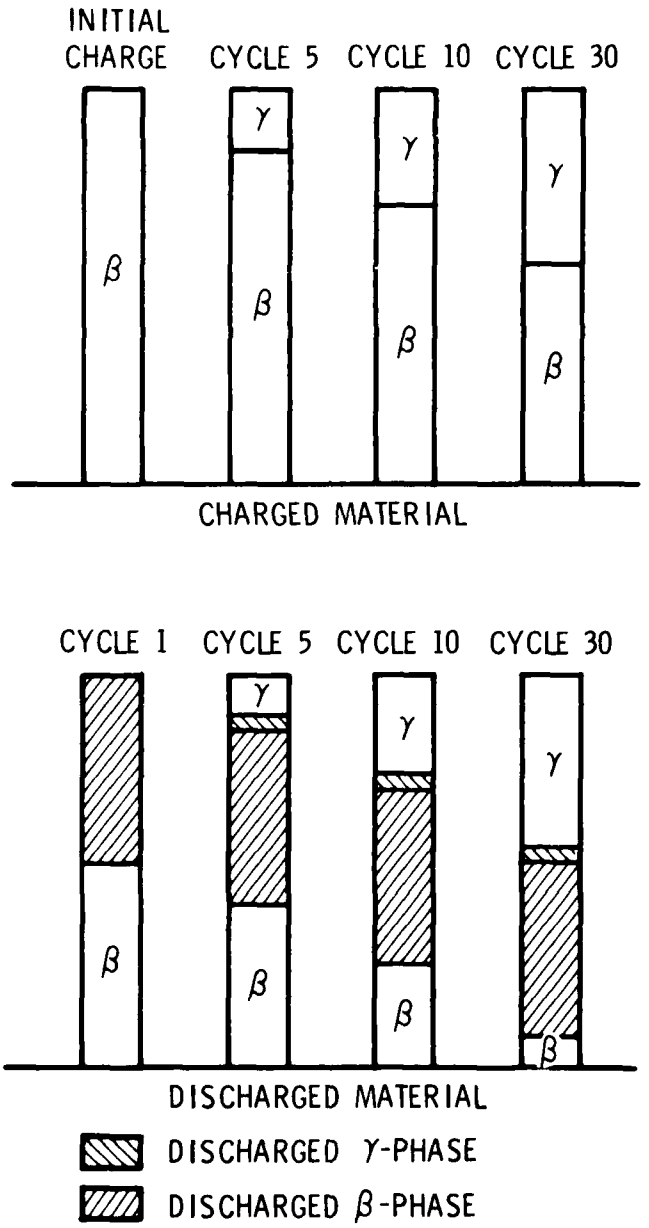

Figure 11. Pictorial representation of how a phase separation may occur in the Ni electrode upon cycling

of the β-NiOOH, and the lower plateau results from discharge of a γ-NiOOH enriched material.

The voltage losses reported here for the NiCd cell are assumed to arise predominantly from the Ni electrode, as the results employing a reference electrode appear to indicate. The change in potential realized after cycling contains both current-independent and current-dependent contributions as indicated by Eq. (2). A change in phase composition of the charged active materials can account for the roughly 20-mV change typically observed in the open-circuit potential. The E_o values for discharge of the γ- NiOOH to α-$Ni(OH)_2$ and the β-NiOOH to β-$Ni(OH)_2$ have been reported[10] to be 1.3179 and 1.3688 V, respectively, versus NHE. The change in E_o of about 20 mV most likely reflects changes in mixed potentials of these phases. From Fig. 6 it is concluded that after extensive cycling much of the increase in ΔV results from increasing overpotential rather than from continued decreases in the open-circuit potential. This conclusion is based on the observation that voltage losses of up to 65 mV have been observed to occur and to continue to increase monotonically after several hundred cycles, while the maximum change expected for the open-circuit potential[10] is less than about 60 mV. These results suggest that the initial voltage losses that occur rapidly during the first 20 to 30 cycles are dominated by changes in open-circuit potential, and that the changes that continue more slowly over the long term result from overpotentials associated with the morphology and physical structures of the crystalline phases at the electrode surfaces. The form of this current-overpotential relationship is given by curve C of Fig. 4 and appears likely to result from a combination of increased electronic resistance and increased resistance to proton diffusion in the NiOOH lattice.[6,7] The steady-state resistance arising from proton diffusion is to a first approximation inversely proportional to the current squared,[16] which can account for the sharply curved function in curve C of Fig. 4 at low currents. At high currents the current-overpotential relationship approaches linearity as the effects of increased electronic resistance become dominant.

The charge-discharge reactions at the Ni electrode [Eq. (1)] are generally considered to occur in the solid state. In such a case the

morphology of the active material deposits is not likely to undergo rapid change in terms of growth or physical migration (a very slow long-term swelling is often observed in Ni electrodes). When a separation of phases occurs in the active material it is possible, and in fact quite likely, that the interface of each individual phase with the electrolyte may be substantially altered as such phase separation develops. This kind of interfacial change may be thought of in terms of the crystallites of active material that comprise each phase forming a structurally inhomogeneous distribution over the electrode surfaces. Phase separation will, therefore, decrease the active surface area of the initial phase, while the total active electrode surface area remains relatively unchanged. These changes will create nonuniformities in the current and potential distribution throughout the electrode, and are therefore likely to increase the overpotential at the Ni electrode. Greater overpotentials may be caused by the increased local current densities on the electrode, as well as by differences in the rates of proton transport in the separated phases. The curvature in the I/V plot (curve C of Fig. 4) at lower currents is qualitatively consistent with the behavior expected for either a transport process or a nonuniform current distribution.

The loss of potential was found to be relatively insensitive to the depth of discharge or the amount of charge return used during cycling. The potential loss was found to depend most strongly on the number of charge-discharge cycles, and the potential was only depressed significantly during discharge of the uncycled material. It was also found that the charge and discharge currents at which the cell was cycled were quite important in determining the rate of voltage loss. When cycled at both low charge and discharge currents, the cell voltage during the final discharge was depressed much more rapidly than when higher cycling currents were used. These results are consistent with the development of phase separation during cycling. For high charge or discharge currents, the charge and discharge processes are less specific in terms of each phase, i.e., nonuniformities in current are less pronounced at higher currents. At low currents the charge and discharge reactions are much more phase specific, with the result being to separate the

active material in terms of phase composition as the Ni electrode is cycled. This situation is the solid-state analog to crystallization from solution where a high growth rate leads to finely divided crystallites interspersed throughout the liquid phase, rather than a few large crystals for low growth rates. In this way the high- and low-rate conditions give rise to dramatically different interfacial areas between the two phases that are undergoing separation.

The recovery of performance that is associated with reconditioning may be regarded as involving the discharge of both phases to a common material. This material is likely to be β-$Ni(OH)_2$ since on recharge the resulting β-NiOOH discharges at a higher potential than γ-NiOOH. Any discharged α-phase can undergo a slow discharge to β-$Ni(OH)_2$ during reconditioning by a process which has been reported in the literature.[10] This process destroys any preexisting phase separation since it puts all the active material in a common phase, β-$Ni(OH)_2$, which may then be recharged.

These results suggest several factors to be considered in cell design and testing. While the specific results obtained here are expected to depend on the particular cell design and should not be quantitatively applied to other designs, the general concepts should be generally applicable to Ni electrodes. It is indicated that the substantial voltage losses realized during long-term cycling are due to modifications of the structure and effective area of the β-NiOOH/electrolyte interface, whereas the short-term losses arise more from changes in the equilibrium potential of the electrode as its phase composition changes. The long-term losses in voltage should therefore be quite sensitive to electrode design parameters such as the relative crystallite dimensions and the typical distances between the current collector and the electrolyte interface. The process by which the active material is impregnated into the current collector should therefore be critical. Indeed, this may be one reason for some of the differences in performance associated with electrochemically impregnated plates. The dependence of voltage losses on charge and discharge rates suggests that these rates should be made as high as possible within the constraints of a given battery system, as long as high-rate overcharge or overcharge at elevated

temperatures are avoided, since these conditions can cause irreversible degradation of the NiCd cell performance. The results also suggest that even a high-rate discharge can provide effective reconditioning in terms of raising the cell potential. However, the capacity that is not discharged during a high-rate reconditioning discharge is likely to remain unavailable, whereas a low-rate reconditioning discharge will recover this capacity, as well as raise the cell potential.

V. CONCLUSIONS

The losses in voltage occurring in a NiCd cell that is repetitively cycled have been measured under a variety of conditions. The voltage changes appear to arise predominantly from changes at the Ni electrode, which undergoes a separation of the active material into two phases. The phase separation changes the open-circuit potential of the cell as a function of depth of discharge. The distribution of the phases appears to be significant in determining the overpotential for discharge of the Ni electrode.

REFERENCES

1. W. R. Scott and D. Rusta, Sealed-Cell Nickel-Cadmium Battery Applications Manual, NASA NAS5-23514, 5 May 1978, pp. 4-120.

2. Y. Okinaka and C. M. Whitehurst, J. Electrochem. Soc. 117, 583 (1970).

3. F. G. Will and H. J. Hess, J. Electrochem. Soc. 120, 1 (1973).

4. D. Chua and R. J. Diefendorf, "Effect of Electrode Structures on Capacity of Sealed Cells During Cycling," 25th Power Sources Symposium, pp. 52-55, 1972.

5. R. Jasinski, High Energy Batteries, Plenum Press, N.Y., 1967.

6. D. M. MacArthur, J. Electrochem. Soc. 117, 422 (1970).

7. D. M. MacArthur, J. Electrochem. Soc. 117, 729 (1970).

8. H. Bode, K. Dehmelt, and J. Witte, Electrochimica Acta 11, 1079 (1966).

9. P. C. Milner and U. B. Thomas, Advances in Electrochemistry and Electrochemical Engineering, Vol. 5, Interscience, New York, 1967, p. 20.

10. R. Barnard, C. F. Randell, and F. L. Tye, J. Appl. Electrochem. 10, 127 (1980).

11. J. P. Harivel et al., Power Sources, D. H. Collins, ed., Pergamon Press, 1966.

12. D. Tuomi, J. Electrochem. Soc. 112, 1 (1965).

13. R. Barnard, G. T. Crickmore, J. A. Lee, and F. L. Tye, J. Appl. Electrochem. 10, 61 (1980).

14. R. Barnard, C. F. Randell, and F. L. Tye, J. Appl. Electrochem. 10, 109 (1980).

15. R. S. Schrebler Guzman, J. R. Vilche, and A. J. Arvia, J. Appl. Electrochem. 9, 183 (1979).

16. A. H. Zimmerman, M. R. Martinelli, M. C. Janecki, and C. C. Badcock, submitted for publication, J. Electrochem. Soc.

LABORATORY OPERATIONS

The Laboratory Operations of The Aerospace Corporation is conducting experimental and theoretical investigations necessary for the evaluation and application of scientific advances to new military concepts and systems. Versatility and flexibility have been developed to a high degree by the laboratory personnel in dealing with the many problems encountered in the Nation's rapidly developing space systems. Expertise in the latest scientific developments is vital to the accomplishment of tasks related to these problems. The laboratories that contribute to this research are:

Aerophysics Laboratory: Aerodynamics; fluid dynamics; plasmadynamics; chemical kinetics; engineering mechanics; flight dynamics; heat transfer; high-power gas lasers, continuous and pulsed, IR, visible, UV; laser physics; laser resonator optics; laser effects and countermeasures.

Chemistry and Physics Laboratory: Atmospheric reactions and optical backgrounds; radiative transfer and atmospheric transmission; thermal and state-specific reaction rates in rocket plumes; chemical thermodynamics and propulsion chemistry; laser isotope separation; chemistry and physics of particles; space environmental and contamination effects on spacecraft materials; lubrication; surface chemistry of insulators and conductors; cathode materials; sensor materials and sensor optics; applied laser spectroscopy; atomic frequency standards; pollution and toxic materials monitoring.

Electronics Research Laboratory: Electromagnetic theory and propagation phenomena; microwave and semiconductor devices and integrated circuits; quantum electronics, lasers, and electro-optics; communication sciences, applied electronics, superconducting and electronic device physics; millimeter-wave and far-infrared technology.

Materials Sciences Laboratory: Development of new materials; composite materials; graphite and ceramics; polymeric materials; weapons effects and hardened materials; materials for electronic devices; dimensionally stable materials; chemical and structural analyses; stress corrosion; fatigue of metals.

Space Sciences Laboratory: Atmospheric and ionospheric physics, radiation from the atmosphere, density and composition of the atmosphere, aurorae and airglow; magnetospheric physics, cosmic rays, generation and propagation of plasma waves in the magnetosphere; solar physics, x-ray astronomy; the effects of nuclear explosions, magnetic storms, and solar activity on the earth's atmosphere, ionosphere, and magnetosphere; the effects of optical, electromagnetic, and particulate radiations in space on space systems.